RESEARCH ARTICLE
doi: 10.2306/scienceasia1513-1874.2025.054

ScienceAsia 51 (3): 2025: ID 2025054: **1–9**

Differential effects of chronic intermittent hypobaric hypoxia on healthy and metabolic syndrome mice through liver tissue proteomic analysis

Cheng Wang[a], Wei Zhang[a], Donghai Zhao[a], Pengyan Ji[a], Ying Chang[b], Dongfang Zhang[a], Xinyu Jiang[a], Mengxin Yu[a], Chunlian Du[b], Yuling Qiu[b], Yingxin Zhang[b], Lianhai Jin[a,*], Chunhong Sui[b,*]

[a] School of Basic Medical Sciences, Jilin Medical University, Jilin 132013 China
[b] School of Pharmacy, Jilin Medical University, Jilin 132013 China

*Corresponding authors, e-mail: lh_jin72@163.com, suichunhong@163.com

Received 29 Aug 2024, Accepted 4 Jun 2025
Available online 29 Jun 2025

ABSTRACT: This study aimed to explore the differences in the effects of chronic intermittent hypobaric hypoxia (CIHH) on healthy and metabolic syndrome (MetS) mice through proteomic analysis of liver tissue. Male C57BL/6J mice were divided into four groups: CON (healthy mice), CIHH (healthy mice exposed to CIHH), MetS (MetS mice), and MetS+CIHH (MetS mice exposed to CIHH). Mice in the MetS and MetS+CIHH groups were used to develop a MetS model induced by a 16-week high-fat diet and 10% fructose water feeding. Then, mice in the CIHH and MetS+CIHH groups were treated with CIHH (simulating 5000-m altitude for 28 days, 6 h daily). MetS diagnostic criteria were routinely measured. Protein expression related to the hypoxia-inducible factor (HIF)-1 signaling pathway was assayed by Western blotting. Quantitative proteomic analysis was performed by mass spectrometry. CIHH significantly improved body weight, abdominal circumference, Lee's index, systolic blood pressure, fasting blood glucose, insulin resistance, triglycerides, total cholesterol, low-density lipoprotein cholesterol, and high-density lipoprotein cholesterol in MetS mice, while these indicators had no statistical difference in healthy mice before and after CIHH treatment. HIF-1α expression in the liver tissue was up-regulated only in MetS mice treated with CIHH. Proteomic analysis revealed disparities in the characteristics of differentially expressed proteins between healthy and MetS mice under CIHH. In summary, CIHH exhibited a significant capacity to improve MetS symptoms by up-regulating HIF-1α expression and activating multiple metabolic and signaling pathways in MetS mice. However, the effects of CIHH on healthy mice remained minimal.

KEYWORDS: chronic intermittent hypobaric hypoxia, metabolic syndrome, liver tissue, proteomics

INTRODUCTION

Metabolic syndrome (MetS) is a complex disorder, characterized by a cluster of metabolic abnormalities involving carbohydrates, lipids, proteins, and other substances in the body [1]. The pathophysiological features of MetS include obesity, hypertension, hyperglycemia, hypertriglyceridemia, hypercholesterolemia, and low levels of high-density lipoprotein cholesterol (HDL-C) [2]. MetS is a risk factor that could significantly increase the prevalence of insulin resistance, type 2 diabetes mellitus, atherosclerosis, cardiocerebral vascular disease, dyslipidemia, nonalcoholic fatty liver disease, gallstone disease, and other comorbidities [3]. According to clinical experiments and epidemiological investigations, the prevalence of MetS has been increasing gradually [4]. Therefore, the prevention and treatment of MetS have become urgent public health issues that require immediate attention. Currently, there is no widely recognized medical solution for MetS [5]. Drug therapy is simply aimed at reducing the harm of MetS comorbidities through hypoglycemic, hypolipidemic, and anti-hypertensive drugs, which are tailored to address the specific needs of each individual patient. Furthermore, the effective strategies for managing potential risk factors associated with MetS are lifestyle changes, which include reducing energy intake, increasing physical activity, quitting smoking, limiting alcohol consumption, and abandoning sedentary habits.

Intermittent hypoxia is a state in which the one, whether it is a cell line, tissue, organ, or whole individual, is exposed alternatively to conditions between hypoxia and normoxia [6]. The consequences of intermittent hypoxia exposure on MetS are entirely different, either harmful or beneficial, which may depend on a variety of factors, such as the change of oxygen concentration, duration, and frequency of hypoxic conditions. There are two opposite views on the role of intermittent hypoxia on MetS, primarily due to the different ways in which intermittent hypoxia conditions are formed. One is the breathing pauses that occur in obstructive sleep apnea. Intermittent hypoxia caused by insufficient ventilation has been considered to be an important risk factor, which can exacerbate varied disorders and diseases induced by MetS [7, 8]. The other is chronic intermittent hypobaric hypoxia (CIHH), a promising non-pharmacological approach that enables tested subjects to undergo regular and periodic exposures in the well-controlled conditions

of hypobaric hypoxia interspersed with normobaric normoxia [9]. CIHH was employed in sports and high-altitude medicine, initially aimed at enhancing the aerobic capacity of athletes or accelerating the altitude acclimatization response in alpinists, and then its novel biomedical applications have gradually expanded [10]. Some experimental evidence has demonstrated that CIHH can alleviate symptoms of MetS and its comorbidities, such as decreasing high blood sugar, relieving dyslipidemia, improving insulin resistance, reducing liver damage, preserving vascular endothelium, and correcting arrhythmia [11–13]. In general, the potential protective role of CIHH may be based on a process termed as CIHH conditioning hormesis, which is an inherent adaptive defense reaction, or rather a resilience derived from powerful endogenous adaptation [14]. However, a full understanding of the underlying mechanism by which CIHH benefits MetS is not yet at hand. Recent studies using animal models have demonstrated that the effect of CIHH on MetS may be involved in a range of intricate processes. The symptoms of obesity, hypertension, glucose and lipid metabolism disorders, reduced insulin sensitivity and glucose tolerance, elevated inflammatory factors, liver tissue morphology and functional damage in MS rats can be improved by CIHH, which may be attributed to over-expressed adiponectin [15], augmented autophagy/ferritinophagy [12, 16] and alleviated endoplasmic reticulum stress [17]. CIHH can regulate the proportion of Firmicutes/Bacteroidetes in gut microbiota, thereby suppressing fat absorption and excessive short-chain fatty acid production, ultimately alleviating fat accumulation [18]. These coordinated adaptations may be related to the hypoxia-inducible factor (HIF)-1 signaling pathway activated by CIHH [19]. In addition, the liver-specific physiological relevance to metabolic health has highlighted the therapeutic potential of CIHH-mediated improvements to MetS. In liver tissue, CIHH significantly reduces the levels of lipid peroxidation, malondialdehyde, aspartate aminotransferase and alanine aminotransferase, enhances activities of glutathione peroxidase and superoxide dismutase, thereby mitigating oxidative stress and suppressing ferroptosis, reversing hepatic steatosis, fibrosis, and inflammation [16].

Proteomics is an integrated research area that focuses on the study of the composition, localization, expression, alteration, interaction, and collaboration of proteins in biological specimens [20]. Proteomic analysis based on mass spectrometry can achieve a large-scale identification and quantification of proteins and has been widely conducted for exploring pathogenesis, searching for diagnostic biomarkers, and screening drug targets [21]. With its systematization, dynamics and high sensitivity, proteomics technology can comprehensively analyze the molecular network of CIHH regulating MetS, and reveal its multi-target mechanism from the level of protein expression, modification and interaction. Therefore, proteomic methods are well suited for a comprehensive preliminary exploration of the impact of CIHH on MetS, providing key technical support for an understanding of the underlying mechanisms for further investigation. This study aimed to employ liver tissue proteomic analysis to investigate the difference in characterization of proteomic profiling between healthy and MetS mice following CIHH treatment, thereby clarifying the underlying mechanism of CIHH-mediated alleviation of MetS symptoms.

MATERIALS AND METHODS

Reagents

Fructose was purchased from Sinopharm, Shanghai, China. Urea, nicotinamide (NAM), trichloroacetic acid (TCA), tetraethylammonium bromide (TEAB), dithiothreitol (DTT) and iodoacetamide (IAM) were purchased from Sigma-Aldrich, CA, USA. Protease inhibitor cocktail was from Merck Millipore, MA, USA. Trichostatin A (TSA) was from MedChemExpress, NJ, USA. Formic acid was obtained from Fluka, Seelze, Germany. Acetonitrile was from Thermo Fisher Scientific, MA, USA. Glucose assay kit and mouse insulin enzyme-linked immunosorbent assay (ELISA) kit were purchased from Jiancheng, Nanjing, China. Animal tissue total protein extraction kit were purchased from Solarbio, Beijing, China. Gel preparation kit, 10 × Tris-Gly buffer and pre-stained protein marker (10 ∼ 150 kDa) for sodium dodecyl sulfate polyacrylamide gel electrophoresis (SDS-PAGE), 10 × transfer buffer, polyvinylidene fluoride (PVDF) membrane and enhanced chemiluminescence (ECL) kit were purchased from Beyotime, Shanghai, China. Rabbit anti-mouse HIF-1α antibody (1:2000, ab16066), HIF-1β antibody (1:1000, ab239366), prolyl hydroxylase (PHD)2 antibody (1:500, ab226890), PHD3 (1:2000, ab184714), β-actin antibody (1:5000, ab8227) and goat anti-rabbit IgG labeled with horseradish peroxidase (1:2000, ab205718) were purchased from Abcom, MA, USA. Rabbit anti mouse von Hippel Lindau (VHL) antibody (#81292) were from Cell Signaling Technology, MA, USA.

Animal experiments

Forty 4-week-old SPF male C57BL/6J mice, weighing 18 g ± 1 g, were purchased from Changchun Yisi Experimental Animal Technology Co., Ltd., Jilin, China. Every 5 mice were placed in a cage. These mice were kept in controlled conditions with a 12-h light/dark cycle at 24 °C ± 2 °C, relative humidity of 55% ± 10%, room air exchange rate of 18 ± 2 air changes/h, ambient noise <60 dB, and had free access to water and food from 8:00 a.m. to 20:00 p.m. The animal procedures were conducted in compliance with the Animal Management Rule of the Ministry of Health, People's Republic of China (Documentation No. 55, 2001) and the Guide for the Care and Use of Laboratory Animals

adopted and promulgated by the US National Institutes of Health. All experimental protocols were reviewed and approved by the Animal Ethics Committee of Jilin Medical University (No. 2022-KJT-013). Mice were evenly and randomly divided into 4 groups: control (CON), CIHH treatment (CIHH), MetS model (MetS), and MetS model plus CIHH treatment (MetS+CIHH) groups, with 10 mice in each group. The animal experimental protocols were revised according to previous studies [22]. Mice in the CON and CIHH groups were fed with a chow diet and drinking water, while mice in the MetS and MetS+CIHH groups were fed with a high-fat diet and a 10% (wt/vol) fructose aqueous solution. Chow and high-fat diets were purchased from Siping Saino Biotechnology Co., Ltd., Jilin, China (Table S1).

After being continuously fed with different diets for 16 weeks, mice in the CIHH and MetS+CIHH groups were placed in a hypobaric hypoxia cabin together (ZS-DY-HP, Zhongshi Technology, Beijing, China), and were treated by CIHH over 28 days. The protocol of CIHH treatment consisted of daily 6-h hypobaric hypoxia exposures (fasted and water-deprived), with the same normobaric normoxia conditions to the normal feeding environment of mice in the CON and MetS groups maintained during all non-exposure periods (free access to water and food). The hypobaric hypoxia exposures simulated 5,000 m altitude conditions (barometric pressure of 54 kPa, O_2 content of 10.9%), uniform control of simulated altitude lift at 120 ± 10 m/min, and other parameters (temperature, humidity, ambient noise) in the cabin were strictly matched to baseline housing conditions, to ensure that simultaneously changing of barometric pressure and oxygen content were the sole stressors, thereby minimizing potential confounding factors.

Indicators used to verify MetS mice were prescribed by referring to the diagnostic criteria for MetS in humans from the World Health Organization and the National Cholesterol Education Program Adult Treatment Panel III [23]. These indicators were divided into 4 categories as criteria for verifying the MetS mouse model, including (1) obesity, assessed by body weight, abdominal circumference, and Lee's index; (2) hypertension, assessed by systolic blood pressure (SBP); (3) dysglycemia assessed by fasting blood glucose (FBG), areas under curve (AUC) of oral glucose tolerance tests (OGTT), and homeostasis model assessment for insulin resistance (HOMA-IR); (4) dyslipidemia, assessed by serum triglycerides (TG), total cholesterol (TC), low-density lipoprotein cholesterol (LDL-C), and high-density lipoprotein cholesterol (HDL-C). It was affirmed as abnormal that the difference between the individual value and the average value of the CON group >1.2 times in the indicators [24]. MetS was considered when at least three of the above criteria were met, with abnormal changes observed in at least one indicator for each criterion. Mice that did not meet these criteria were excluded.

MetS characteristics evaluation

Indicators utilized for evaluating the MetS characteristics in mice were also employed to investigate the effect of CIHH on MetS. The degree of obesity was quantified through body weight, abdominal circumference, and Lee's index. Body weight, body length, and abdominal circumference were measured routinely. Lee's index was calculated as the $[\text{body weight (g)} \times 10^3]^{1/3}/\text{body length (cm)}$ formula [25]. SBP was measured using a non-invasive tail cuff blood pressure machine (MRBP-R01, IITC Life Sciences, CA, USA). FBG was measured with whole blood collected from the tail tip using a blood glucometer (590, Yuwell Medical Equipment & Supply, Jiangsu, China). Mice in each group were fasted for 12 h after the last CIHH treatment, followed by OGTT and AUC calculation [26]. Fasting serum glucose (FSG) and fasting serum insulin (FSI) were measured using a glucose assay kit and a mouse insulin ELISA kit, respectively. Subsequently, HOMA-IR was calculated as: HOMA-IR = FSG (mmol/l) × FSI (mU/l)/22.5 formula [27]. TG, TC, HDL-C, and LDL-C levels in the serum of mice were used to analyze lipid metabolism and were measured using an automatic veterinary biochemical analyzer (LABOSPECT008, Hitachi, Tokyo, Japan).

Western blotting

Proteins in mouse liver were extracted using an animal tissue total protein extraction kit. 30 μg protein from each sample was separated by 12% SDS-PAGE and transferred to the PVDF membrane. The PVDF membrane was incubated with specific primary Abs (HIF-1α, HIF-1β, PHD2, PHD3, VHL), and then with the secondary antibody (goat anti-rabbit IgG labeled with horseradish peroxidase). The protein bands were detected by ECL reaction and visualized with a gelatum/irradiance image analysis system (ChemiDoc XRS+, Bio-Rad, CA, USA).

Quantitative proteomics analysis

A total of 12 liver tissue samples, obtained from male C57BL/6J mice in the CON, CIHH, MetS, and MetS+CIHH groups with 3 mice per group, were used for a proteomic analysis. The quantitative proteomic was completed using the 4D-FastDIA method by Hangzhou Jingjie Co., Ltd., China. Each mouse liver tissue sample weighing about 40 mg was cryopulverized in liquid nitrogen and resuspended in 4 volumes of lysis buffer (8 mol/l urea, 1% protease inhibitor cocktail, 3 μmol/l TSA, 50 mmol/l NAM), and sonicated on ice for 3 min. Lysates were centrifuged at 12,000×g for 10 min at 4 °C. Proteins in supernatant were collected and quantified via bicinchoninic acid (BCA) assay. Protein solutions were adjusted to final concentration of 20% (m/v) with TCA, incubated at 4 °C for 2 h. The precipitated protein was centrifuged at 4,500×g for 5 min at 4 °C,

washed with pre-cooled acetone 3 times, and briefly dried. Proteins were redissolved in 200 mmol/l TEAB, and digested overnight at 37 °C with trypsin at a 1:50 (w/w) ratio. The obtained peptides were reduced with 5 mmol/l DTT at 56 °C for 30 min, and alkylated with 11 mmol/l IAM in the dark at room temperature for 15 min, and desalted using a solid-phase extraction (SPE) column (Strata-X, Phenomenex, Tianjin, China). Carbamidomethyl of cysteine was specified as a fixed modification. Acetylation of the protein N-terminal, and oxidation of methionine were specified as variable modifications. Peptides were separated using an ultra-high performance liquid chromatograph (UHPLC) system (NanoElute, Bruker Daltonics, MA, USA) with a reversed-phase column (25 cm length, 100 µm i.d.) at a constant flow rate of 500 nl/min. The mobile phase consisted of solvent A (0.1% formic acid, 2% acetonitrile/in water) and solvent B (0.1% formic acid in acetonitrile), with gradient elution: 6%∼24% B (0∼24 min), 24%∼35% B (24∼32 min), 35% 80% B (32∼36 min), and 80% B (36∼40 min). Time of flight mass spectrometry (TOF-MS) analysis was performed in data-independent parallel accumulation serial fragmentation (PASEF) mode (1.75 kV electrospray voltage), acquiring 20 MS/MS scans per cycle (400∼850 m/z, 7 m/z isolation window) across a full MS range (300∼1500 m/z). The MS data were searched against Mus_musculus_10090_SP_20230103.fasta (17,132 entries) concatenated with the reverse decoy database. After the database search, the quality of MS data and protein samples was assessed, the protein expression levels were quantified, and the repeatability and dispersion of the sample data were evaluated using Pearson's correlation coefficient (PCC), principal component analysis (PCA), relative standard deviation (RSD), and Log10 intensity dispersion. All proteins were screened by a one-way analysis of variance (ANOVA), with those having a p-value < 0.05 identified as differentially expressed proteins (DEPs). DEPs were annotated through a variety of software and databases (Table S2). Classification, enrichment, and cluster analysis of DEPs were conducted in aspects of biological process, cellular component, molecular function, subcellular localization, and pathway.

Statistical analysis

Statistical analyses were performed with SPSS 23.0 software. The data were expressed as mean ± standard deviation (mean ± SD), and differences among groups were analyzed with a one-way analysis of variance (ANOVA) with least significant difference (LSD) post-hoc test. Probability (p) values less than 0.05 were considered to be statistically significant.

RESULTS

Effects of CIHH on physiological and biochemical indicators in healthy and MetS mice

After the desired treatments for each group of mice, indicators related to the MetS symptoms were detected and calculated, including body weight, body length, Lee's index, abdominal circumference, SBP, AUC from OGTT, FBG, FSG, FSI, HOMA-IR, TG, TC, HDL-C, and LDL-C (Table 1). The body weight was periodically measured once a week (Fig. 1A). FBG was measured in each group every 4 days during the entire 28-day CIHH treatment period (Fig. 1B). Glucose tolerance curves of OGTT were plotted based on the blood glucose concentration measured at various time points (Fig. 1C). The results of the above experiment show that there was no statistical difference in indicators related to the MetS symptoms of mice between the CON group and the CIHH group ($p > 0.05$). Compared with the CON group, significant changes were observed in various indicators of mice in the MetS and MetS+CIHH groups, with an increase in body weight, Lee's index, abdominal circumference, SBP, AUC, FSG, FSI, TG, TC, HDL-C, and a decrease in LDL-C ($p < 0.05$). Compared with the MetS group, mice in the MetS+CIHH group exhibited a significant relief ($p < 0.05$).

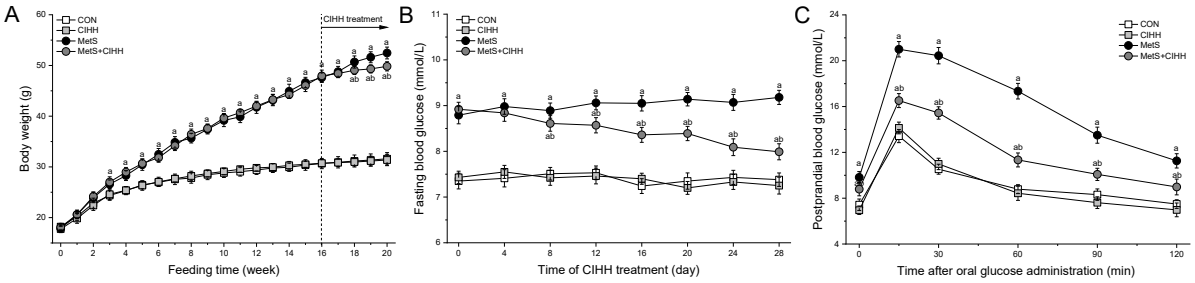

Fig. 1 Effects of CIHH on body weight, fasting blood glucose and glucose tolerence in healthy and MetS mice. (A) Body weight changes throughout the entire experimental period. (B) FBG levels during CIHH treatment. (C) OGTT. Data were expressed as mean ± SD, $n = 10$ in each group. Different letters indicate a significant difference, [a] $p < 0.05$, compared with the CON group; [b] $p < 0.05$, compared with the MetS group.

Table 1 Effects of CIHH on physiological and biochemical indicators in healthy and MetS mice.

Indicator	Group			
	CON	CIHH	MetS	MetS+CIHH
Lee' index	3.36 ± 0.12	3.40 ± 0.14	3.87 ± 0.13[a]	3.71 ± 0.15[ab]
Abdominal circumference (cm)	8.27 ± 0.39	8.15 ± 0.38	9.53 ± 0.42[a]	9.01 ± 0.47[ab]
SBP (mmHg)	112.79 ± 10.75	117.70 ± 11.14	147.94 ± 12.63[a]	128.13 ± 11.67[ab]
AUC (mmol/l × min)	1119.30 ± 29.81	1097.25 ± 34.47	1922.64 ± 77.78[a]	1438.42 ± 50.60[ab]
FSG (mmol/l)	6.84 ± 0.89	6.59 ± 0.97	10.68 ± 1.35[a]	9.21 ± 1.26[ab]
FSI (mU/l)	23.58 ± 3.34	22.24 ± 3.98	34.87 ± 4.03[a]	29.47 ± 4.49[ab]
HOMA-IR	7.12 ± 1.08	6.46 ± 1.23	16.60 ± 3.04[a]	12.07 ± 2.63[ab]
Serum TG (mmol/l)	1.24 ± 0.16	1.10 ± 0.18	1.83 ± 0.20[a]	1.47 ± 0.19[ab]
Serum TC (mmol/l)	2.75 ± 0.33	2.68 ± 0.29	4.13 ± 0.31[a]	3.62 ± 0.28[ab]
Serum LDL-C (mmol/l)	0.26 ± 0.03	0.25 ± 0.02	0.42 ± 0.04[a]	0.32 ± 0.03[ab]
Serum HDL-C (mmol/l)	1.81 ± 0.15	1.76 ± 0.12	1.29 ± 0.13[a]	1.45 ± 0.14[ab]

Data were expressed as mean ± SD, $n = 10$ in each group. Different letters indicate a significant difference, [a] $p < 0.05$, compared with the CON group; [b] $p < 0.05$, compared with the MetS group.

Effects of CIHH on expression of HIF-1 signaling pathway related proteins in healthy and MetS mice

Expression of proteins involved in the HIF-1 signaling pathway, including HIF-1α, HIF-1β, PHD2, PHD3, and VHL, was detected using Western blotting (Fig. 2A). The relative expression levels of proteins were equivalent (Fig. 2B). Compared with the CON group, the relative protein expression level of HIF-1α in the liver of mice in the MetS+CIHH group increased significantly ($p < 0.05$), while that in the liver of mice in the CIHH and MetS groups had no statistically significant change ($p > 0.05$).

Effects of CIHH on the liver tissue proteomics in healthy and MetS mice

Protein samples from mouse liver tissue in four groups were subjected to proteome sequencing. The number of identified peptides and proteins was 71,079 and 7,181, respectively, of which 68185 unique peptides and 7,147 comparable proteins were detected. Peptide length is mainly between 7 to 26 amino acids, and the distribution of peptide length and protein molecular weight approximates a Gaussian distribution (Fig. S1A,B). The distribution of the peptide quantity for each protein showed that proteins with more peptide fragments exhibited a lower number. (Fig. S1C). The coverage rate of most proteins was below 30% (Fig. S1D). It indicated that sample preparation was reliable, mass spectrometry detection was stable and reproducible, and the obtained peptide information had a high database matching rate and recognition confidence. A high degree of reproducibility between each sample was observed according to PCC obtained from comparisons of normalized intensity values, indicating that the data were stable and reliable (Fig. S2A). In PCA, sample points in each group were gathered together, accompanied by non-overlapping confidence regions, indicating that the mouse livers in four groups had distinct protein expression signatures (Fig. S2B). The comparison of RSD showed that data between groups had high repeatability (Fig. S2C). The average Log10 intensity values and density distribution curve shapes remained largely unchanged across all samples, indicating samples had high quality and low dispersion (Fig. S2D,E).

1593 proteins were classified into 3 clusters, excluding 5554 proteins designated as not applicable (NA). Expression levels of clustered proteins were observed to be different among groups (Fig. 3A). Then, significant up-regulation and down-regulation DEPs caused by CIHH treatment were screened in healthy mice (CIHH group vs. CON group) and MetS mice (MetS+CIHH group vs. MetS group), respectively (Fig. 3B). 87 DEPs in healthy mice and 438 DEPs in MetS mice were identified. It was found that, following treatment with CIHH, up-regulated DEPs surpassed down-regulated DEPs in healthy mice, in contrast, up-regulated DEPs were less than down-regulated DEPs in MetS mice (Fig. 3C).

Identified proteins were annotated in detail, encompassing GO classification, subcellular localization, the KEGG pathway, Reactome, and WikiPathways (Fig. S3). Based on the annotation data, a comprehensive analysis was conducted using methods of classification, enrichment, and clustering to investigate the functional characteristics of DEPs caused by CIHH treatment in healthy and MetS mice. The top 10 items of the GO classification on "biological process", "cell component", and "molecular function" revealed that DEPs played a pivotal role in diverse metabolic and responsive processes, were involved in the components of various membranes, and mainly exhibited the functions related to the binding of proteins and cyclic compounds, as well as enzymatic catalytic and regulatory activities (Fig. 3D). Analysis of "subcellular localization" showed that DEPs were mainly located in the cytoplasm, nucleus, mitochondria, plasma membrane and extracellular (Fig. 3E). A remarkable finding was the emergence of 12 DEPs within the endoplasmic reticulum of liver samples from CIHH-treated MetS mice, while no DEP was observed in the endoplasmic

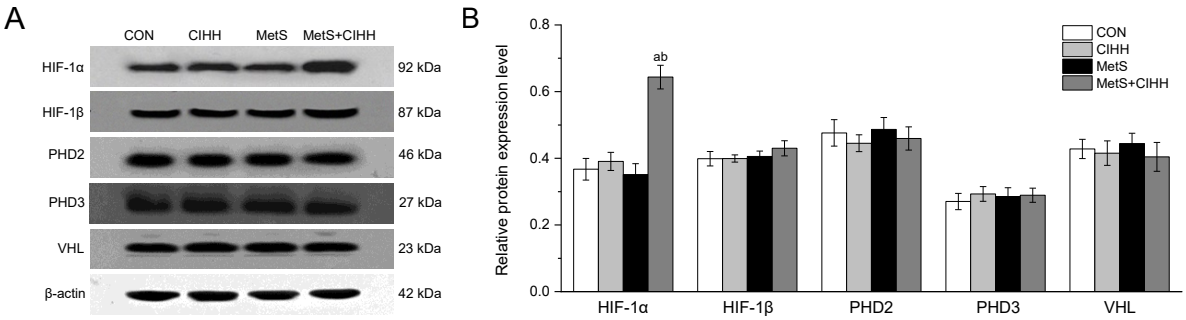

Fig. 2 Effects of CIHH on the expression of HIF-1 signaling pathway related proteins in healthy and MetS mice. (A) Western blot bands. (B) Relative protein expression levels of HIF-1α, HIF-1β, PHD2, PHD3, VHL. β-actin was the endogenous control. Data were expressed as mean ± SD, $n = 3$ in each group. Different letters indicate a significant difference, [a] $p < 0.05$, compared with the CON group; [b] $p < 0.05$, compared with the MetS group.

reticulum of liver samples in healthy mice undergoing the identical CIHH treatment. After cluster analysis, 13 significantly altered metabolic and signaling pathways related to hypobaric hypoxia, glucometabolism, and lipometabolism were revealed in MetS mice, and the same pathways were selected for comparison in healthy mice (Fig. 3F). It was found that there was no statistical change in the corresponding pathways of healthy mice after CIHH treatment, except for pathways of "metabolism of proteins" and "biological oxidations". The number of DEPs involved in each pathway of healthy mice was less than that of MetS mice.

DISCUSSION

The effect of CIHH on healthy and MetS mice was investigated through a series of physiological and biochemical tests and proteomic analyses. During the establishment phase of the MetS mouse model, an obvious distinction was observed in the MetS diagnostic criteria pertaining to obesity, hypertension, dysglycemia, and dyslipidemia in mice fed a high-fat diet and fructose solution, in contrast to mice maintained on a chow diet and water consumption. The successful development of the MetS mouse model served as a pivotal foundation for subsequent experiments. After CIHH treatment, it was found that MetS mice showed significant improvement in indicators related to the MetS symptoms. These results are consistent with previous studies and further confirm the effectiveness of CIHH in improving MetS [11–13, 15, 16, 22].

HIF-1, a pivotal transcription factor containing α and β subunits, serves as a sentinel for detecting variations in oxygen levels in organisms. Under hypoxic circumstances, it undergoes activation, triggering a cascade of physiological and pathological alterations that have profound implications for various biological processes [19]. In MetS mice, HIF-1α expression levels were observed to be significantly elevated following the application of CIHH treatment, suggesting a potential regulatory role in the metabolic profile. To explore the putative mechanisms underlying the beneficial effects of CIHH on MetS, a proteomic study of liver tissue was performed. In the previous proteomics analysis for the functional implications of DEPs in the context of MetS and CIHH [28], some candidate DEPs with biomarker potential were identified, including peroxisome proliferator activated receptor (PPAR), ATP-dependent phosphofructokinase (PFK), hexokinase-2 (HK-2), pyruvate kinase M (PKM), enoyl-CoA hydratase/3-hydroxyacyl-CoA dehydrogenase (EHHADH), sterol regulatory element-binding protein 1 (SREBP1), etc., involving multiple metabolic and signaling pathways such as steroid hormone biosynthesis, arachidonic acid metabolism, fatty acid elongation, glycolysis/gluconeogenesis, PPAR signaling pathway, glutathione metabolism, and HIF-1 signaling pathway, etc. Combining the results of proteomics and molecular biology experiments, the HIF-1 signaling pathway was confirmed as a critical regulatory node regulating metabolic adaptations in response to CIHH exposure. Elevated HIF-1α protein may interact with the PPAR and other signaling pathway to regulate nutrient metabolism, such as enhancing glycolysis, inhibiting gluconeogenesis and fatty acid oxidation, thereby maintaining blood glucose homeostasis and alleviating insulin resistance. Further analysis of proteomics revealed these DEPs had been verified to implicate a broad range of biological processes, cellular components, molecular functions, subcellular localization, and metabolic and signaling pathways, indicating that CIHH might ameliorate MetS symptoms through the intricate regulation of protein expression at multiple hierarchical levels. Specifically, DEPs in glucometabolism, such as PFK, HK-2, and PKM, demonstrated coordinated regulation of glycolysis and gluconeogenesis, enhancing insulin sensitivity and mitigating insulin resistance. DEPs in lipometabolism, such as SREBP1 and EHHADH, were participated in modulating unsaturated fatty acid catabolism and fatty acid elongation, contributing to alleviate lipid metabolism dysfunction. Additionally, DEPs involved in oxidative

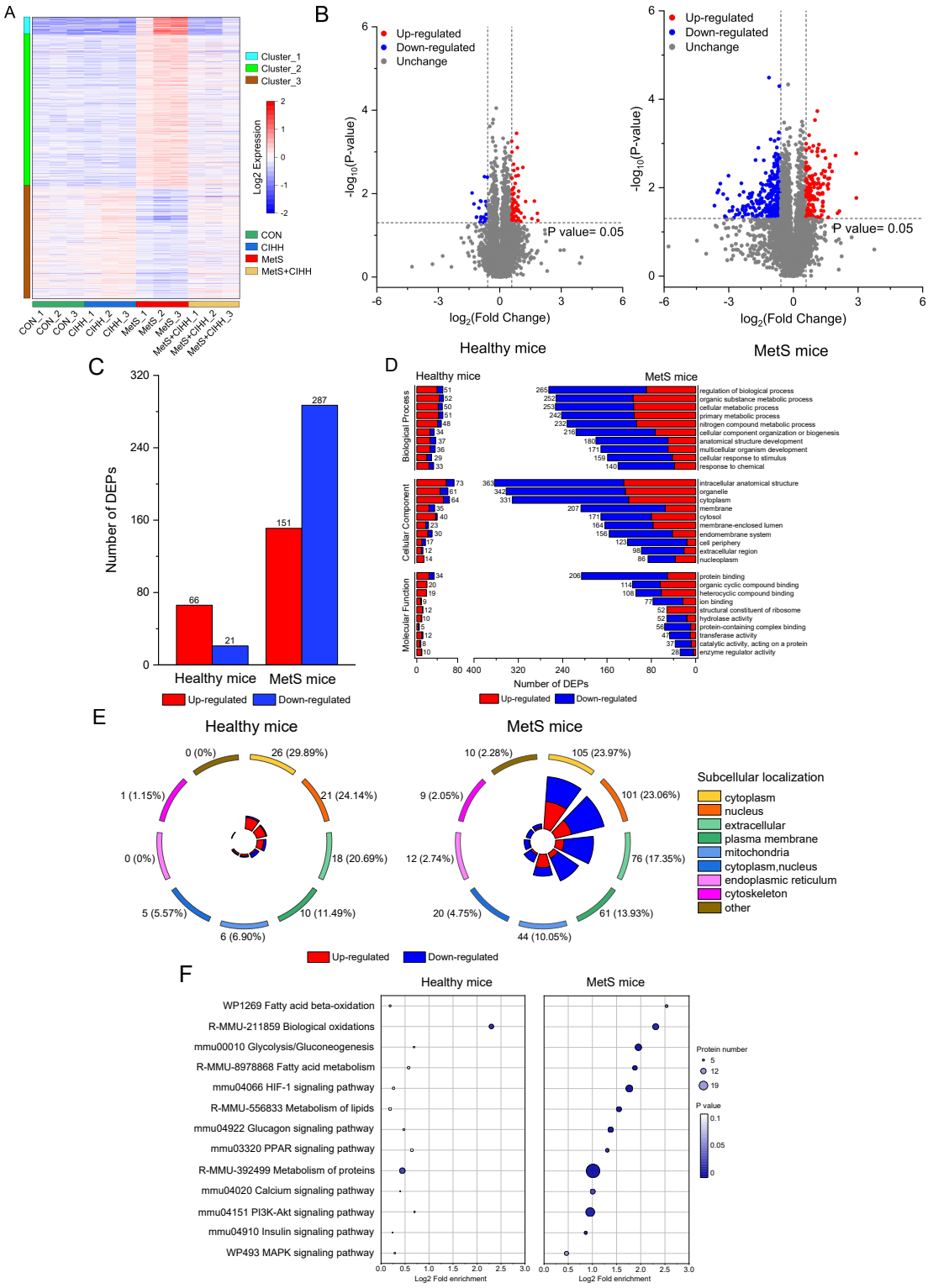

Fig. 3 Effects of CIHH on the liver tissue proteomics in healthy and MetS mice. (A) Heat map of DEPs analyzed by ANOVA in each sample. (B) Volcano plots of the DEPs. (C) Numbers of up-regulated and down-regulated DEPs. (D) Top 10 GO items of "biological process", "cell component", and "molecular function". (E) Subcellular localization. (F) Metabolism and signaling pathways. HIF: hypoxia inducible factor, PPAR: peroxisome proliferator activated receptor, PI3K: phosphotylinositol 3 kinase, Akt: protein kinase B, MAPK: mitogen-activated protein kinase.

stress, endoplasmic reticulum stress and inflammatory collectively attenuated hepatic dysfunction, thereby further improving the symptoms of MetS.

Notably, an intriguing phenomenon appeared, which was that CIHH had a distinct improvement function on MetS mice but displayed negligible impacts on healthy mice. In this study, the results of various indicators used for diagnosing MetS confirmed this phenomenon. Previous studies also showed that other indicators had similar phenomena in healthy and MetS rats. For example, CIHH could reduce the abnormally increased liver index, aspartate aminotransferase, alanine aminotransferase, and protein expression of interleukin-1β, and tumor necrosis factor-α in MetS rats, yet the effect of CIHH on these indicators had no significant change in healthy rats [11, 15]. Furthermore, upon exposure to the same conditions of CIHH, the expression of HIF-1α in the liver tissue of MetS mice was observed to be significantly increased, whereas it remained unaltered in healthy mice. This finding aligns with previous reports regarding HIF-1α expression in normal skin and keloid tissue [29]. By comparing the differences in the liver tissue protein expression between MetS and healthy mice treated with CIHH through proteomics analysis, the potential molecular mechanism underlying the efficacy of CIHH in improving MetS was revealed. CIHH treatment elicited more DEPs in MetS mice than in healthy mice, indicating that there exist distinct differences in the effects of CIHH on MetS and healthy mice from the perspective of protein expression profiles. These results suggested that CIHH had a specific therapeutic effect on MetS mice rather than a general physiological impact. This specificity could potentially be attributed to the distinct metabolic status exhibited between MetS and healthy mice. The metabolic and signaling pathways in the liver tissue of MetS mice were more active as a result of a variety of metabolic disorders, potentially explaining why MetS mice were more susceptible to CIHH treatment. Conversely, in the liver tissue of healthy mice, owing to the relatively stable metabolic homeostasis, CIHH elicited a negligible response.

A new avenue was provided for the clinical application of CIHH as a therapeutic modality in the management of MetS. However, potential confounding factors warrant consideration. Specifically, systemic stress responses, such as activation of the hypothalamic-pituitary-adrenal axis and oxidative stress pathways, could influence liver function due to possible transient dysfunction or inflammatory effects [30]. Furthermore, several study design priorities should be emphasized in the future, including implementing a long-term follow-up to evaluate CIHH's sustained efficacy and delayed adverse effects, such as prolonged hormonal dysregulation or organ-adaptation fatigue, and refining hypoxic animal models by evaluating species-specific responses and reproducibility, and standardizing strict environmental condition controls of CIHH treatment to ensure data reliability. Currently, hypobaric hypoxic cabins are commonly utilized in CIHH treatment, and the cabin's condition parameters are typically established by simulating a specific high-altitude environment that is suitable for survival [31]. The therapeutic benefits of training using hypobaric hypoxic cabins have been validated by extensive preclinical animal and clinical human trials [32]. In addition to MetS, CIHH not only demonstrated broad therapeutic potential for diverse pathologies such as diabetes, cardiovascular disease, hypertension, osteoporosis, and neurodegenerative disorders, but also was helpful for some conventional and intensive training in endurance sports programs, including skiing, swimming, and marathon racing [33]. As a non-invasive therapeutic modality, CIHH treatment has potential application value in clinical adjuvant therapy and has gradually evolved into a research focus and potential for wide application prospects.

CONCLUSION

CIHH exhibited a profound improvement in MetS mice, particularly in key indicators encompassing body weight, abdominal circumference, SBP, FBG, HOMA-IR, TG, TC, LDL-C, and HDL-C. Conversely, its effects on healthy mice were negligible. Further Western blotting and proteomic analysis revealed that CIHH upregulated the expression of HIF-1α in the liver tissue of MetS mice, thus activating various metabolic and signaling pathways, thereby improving MetS symptoms. These findings elucidated the underlying mechanism of CIHH in alleviating MetS and indicated the potential specificity of CIHH in alleviating MetS.

Appendix A. Supplementary data

Supplementary data associated with this article can be found at https://dx.doi.org/10.2306/scienceasia1513-1874.2025.054. The proteomic data have been deposited to the ProteomeXchange Consortium via the iProX system with the data set identifier IPX0009216000.

Acknowledgements: This work was supported by the Natural Science Foundation of Jilin Province Science and Technology Development Plan Project (No. YDZJ202301ZYTS160).

REFERENCES

1. Sherling DH, Perumareddi P, Hennekens CH (2017) Metabolic syndrome. *J Cardiovasc Pharmacol Ther* **22**, 365–367.
2. Fahed G, Aoun L, Bou Zerdan M, Allam S, Bou Zerdan M, Bouferraa Y, Assi HI (2022) Metabolic syndrome: updates on pathophysiology and management in 2021. *Int J Mol Sci* **23**, 786.
3. Masenga SK, Kabwe LS, Chakulya M, Kirabo A (2023) Mechanisms of oxidative stress in metabolic syndrome. *Int J Mol Sci* **24**, 7898.
4. Schütte S, Eberhard S, Burger B, Hemmerling M, Rossol S, Stahmeyer JT (2023) Prevalence of metabolic syndrome: analysis based on routine statutory health insurance data. *Inn Med (Heidelb)* **64**, 482–489.

5. Wang HH, Lee DK, Liu M, Portincasa P, Wang DQ (2020) Novel insights into the pathogenesis and management of the metabolic syndrome. *Pediatr Gastroenterol Hepatol Nutr* **23**, 189–230.
6. Panza GS, Burtscher J, Zhao F (2023) Intermittent hypoxia: a call for harmonization in terminology. *J Appl Physiol* **135**, 886–890.
7. Pu JY, Zhao Y, Bai X, Feng T, Lu WQ, Ding LH, Yu Q (2024) Cyclic intermittent hypoxia induces apoptosis through upregulation of lncRNA GAS5 expression in cardiomyocytes. *ScienceAsia* **50**, ID 2024061.
8. Giampá SQC, Lorenzi-Filho G, Drager LF (2023) Obstructive sleep apnea and metabolic syndrome. *Obesity (Silver Spring)* **31**, 900–911.
9. Guo H, Zhao Y, Mu R, Zhang G, Chen S, Cao X, Liu K, Liu Y, et al (2024) The protective effect of chronic intermittent hypobaric hypoxia on preventing the destruction of CD34+ haematopoietic stem cells in aplastic anaemia by modulating the Th1/Th2 balance. *Stem Cell Rev Rep* **20**, 301–312.
10. Viscor G, Torrella JR, Corral L, Ricart A, Javierre C, Pages T, Ventura JL (2018) Physiological and biological responses to short-term intermittent hypobaric hypoxia exposure: from sports and mountain medicine to new biomedical applications. *Front Physiol* **9**, 814.
11. Zhou JJ, Ma HJ, Liu Y, Guan Y, Maslov LN, Li DP, Zhang Y (2015) The anti-arrhythmic effect of chronic intermittent hypobaric hypoxia in rats with metabolic syndrome induced with fructose. *Can J Physiol Pharmacol* **93**, 227–232.
12. Cui F, Hu HF, Guo J, Sun J, Shi M (2020) The effect of autophagy on chronic intermittent hypobaric hypoxia ameliorating liver damage in metabolic syndrome rats. *Front Physiol* **11**, 13.
13. Cui F, Guan Y, Guo J, Tian YM, Hu HF, Zhang XJ, Zhang Y (2018) Chronic intermittent hypobaric hypoxia protects vascular endothelium by ameliorating autophagy in metabolic syndrome rats. *Life Sci* **205**, 145–154.
14. Zhang Q, Zhao W, Li S, Ding Y, Wang Y, Ji X (2023) Intermittent hypoxia conditioning: a potential multi-organ protective therapeutic strategy. *Int J Med Sci* **20**, 1551–1561.
15. Cui F, Mi H, Guan Y, Zhu Y, Wang R, Tian Y, Yang K, Zhang Y (2023) Chronic intermittent hypobaric hypoxia ameliorates vascular reactivity through upregulating adiponectin expression of PVAT in metabolic syndrome rats. *Can J Physiol Pharmacol* **101**, 160–170.
16. Cui F, Mi H, Wang R, Du Y, Li F, Chang S, Su Y, Liu A, et al (2023) The effect of chronic intermittent hypobaric hypoxia improving liver damage in metabolic syndrome rats through ferritinophagy. *Pflugers Arch* **475**, 1251–1263.
17. Yuan F, Teng X, Guo Z, Zhou JJ, Zhang Y, Wang S (2015) Chronic intermittent hypobaric hypoxia ameliorates endoplasmic reticulum stress mediated liver damage induced by fructose in rats. *Life Sci* **121**, 40–45.
18. Tian YM, Guan Y, Tian SY, Yuan F, Zhang L, Zhang Y (2018) Short-term chronic intermittent hypobaric hypoxia alters gut microbiota composition in rats. *Biomed Environ Sci* **31**, 898–901.
19. Taylor CT, Scholz CC (2022) The effect of HIF on metabolism and immunity. *Nat Rev Nephrol* **18**, 573–587.
20. Bader JM, Albrecht V, Mann M (2023) MS-based proteomics of body fluids: the end of the beginning. *Mol Cell Proteomics* **22**, 100577.
21. Birhanu AG (2023) Mass spectrometry-based proteomics as an emerging tool in clinical laboratories. *Clin Proteomics* **20**, 32.
22. Cui F, Shi M, Hu HF, Tian YM, Zhou CM, Mi HC, Gu S, Guo Z, et al (2022) Adenosine monophosphate-activated protein kinase-mammalian target of rapamycin signaling participates in the protective effect of chronic intermittent hypobaric hypoxia on vascular endothelium of metabolic syndrome rats. *Chin J Physiol* **65**, 53–63.
23. Tarcău BM, Vicaş LG, Filip L, Maghiar F, Şandor M, Pallag A, Jurca T, Mureşan ME, et al (2023) Emerging perspectives on the set of conditions that lead to the emergence of metabolic syndrome. *J Pers Med* **14**, 32.
24. Arellano Buendia AS, Juárez Rojas JG, García-Arroyo F, Aparicio Trejo OE, Sánchez-Muñoz F, Argüello-García R, Sánchez-Lozada LG, Bojalil R, et al (2023) Antioxidant and anti-inflammatory effects of allicin in the kidney of an experimental model of metabolic syndrome. *PeerJ* **11**, e16132.
25. Fu K, Gao X, Hua P, Huang Y, Dong R, Wang M, Li Q, Li Z (2023) Anti-obesity effect of *Angelica keiskei* Jiaosu prepared by yeast fermentation on high-fat diet-fed mice. *Front Nutr* **9**, 1079784.
26. Small L, Ehrlich A, Iversen J, Ashcroft SP, Trošt K, Moritz T, Hartmann B, Holst JJ, et al (2022) Comparative analysis of oral and intraperitoneal glucose tolerance tests in mice. *Mol Metab* **57**, 101440.
27. Sangartit W, Ha KB, Lee ES, Kim HM, Kukongviriyapan U, Lee EY, Chung CH (2021) Tetrahydrocurcumin ameliorates kidney injury and high systolic blood pressure in high-fat diet-induced type 2 diabetic mice. *Endocrinol Metab* **36**, 810–822.
28. Zhang DF, Zhang Y, Zhao Q, He YT, Chang Y, Ji PY, Wang C (2025) Analysis of the pathogenesis of metabolic syndrome based on proteomics of mouse liver tissue. *J Jilin Med Univ* **46**, 241–248.
29. Lei R, Li J, Liu F, Li W, Zhang S, Wang Y, Chu X, Xu J (2019) HIF-1α promotes keloid development through the activation of TGF-β/Smad and TLR4/MyD88/NF-κB pathways. *Cell Cycle* **18**, 3239–3250.
30. Liu J, Xu J, Guan S, Wang W (2024) Effects of different treatments on metabolic syndrome in patients with obstructive sleep apnea: a meta-analysis. *Front Med* **11**, 1354489.
31. Hillman TC, Idnani R, Wilson CG (2022) An inexpensive open-source chamber for controlled hypoxia/hyperoxia exposure. *Front Physiol* **13**, 891005.
32. Nakdimon I, Ben-Ari O (2022) Mitigating risks of altitude chamber training. *Aerosp Med Hum Perform* **93**, 811–815.
33. Mujika I, Sharma AP, Stellingwerff T (2019) Contemporary periodization of altitude training for elite endurance athletes: a narrative review. *Sports Med* **49**, 1651–1669.

Appendix A. Supplementary data

Table S1 Information on feedstuffs on a chow diet and a high-fat diet.

Item		Chow diet	High-fat diet
Energy (kcal/g)		3.85	5.24
Composition (%)			
	Casein	18.86	25.85
	Cystine	0.29	0.38
	Corn starch	29.86	0.00
	Maltodextrin	3.32	16.15
	Sugar	33.18	8.89
	Cellulose	4.75	6.46
	Soybean oil	2.38	3.23
	Lard	1.91	31.66
	Calcium hydrogen phosphate	1.25	1.68
	Calcium carbonate	0.53	0.71
	Potassium citrate	1.57	2.13
	Choline tartrate	0.19	0.26
	vitamin complex	0.96	1.31
	Mineral mixed	0.95	1.29
Energy supply ratio of nutrients (%)			
	Protein	20	20
	Carbohydrates	70	20
	Fat	10	60

Table S2 Information on annotation software.

Function	Software	Database	Notes
GO	eggnog-mapper (v2.1.6)	eggNOG (v5.0.2, http://eggnog5.embl.de/#/app/home)	—
COG/KOG	eggnog-mapper (v2.1.6)	eggNOG (v5.0.2, http://eggnog5.embl.de/#/app/home) NCBI (COG2020, KOG, https://ftp.ncbi.nih.gov/pub/COG/)	—
Protein Domain	PfamScan (v1.6)	pfam (A.hmm-33.1, https://www.ebi.ac.uk/interpro/entry/pfam/#table)	—
KEGG pathway	Diamond (v2.0.11.149)	KAAS (April 3, 2015, http://www.genome.jp/kegg/kaas/) KEGG mapper (v5.0, http://www.kegg.jp/kegg/mapper.html)	Human/Mouse/Rat
		KOBAS (v3.0, http://kobas.cbi.pku.edu.cn/) KEGG mapper (v5.0, http://www.kegg.jp/kegg/mapper.html)	Non-virus
PPI	Diamond (v2.0.11.149)	STRING (v11.5, https://cn.string-db.org/)	Non-virus
Subcellular localization	WolF Psort	(v0.2)	Eukaryote
	PSORTb (v3.0)	—	Prokaryote
Reactome	—	Reactome (https://reactome.org/)	Human/Mouse/Rat
WiKipathways	—	WikiPathways (https://www.wikipathways.org/)	Human/Mouse/Rat
HallMark	—	MSigDB (v2022.1, http://www.gsea-msigdb.org/gsea/msigdb/human/ collections.jsp#H)	Human/Mouse

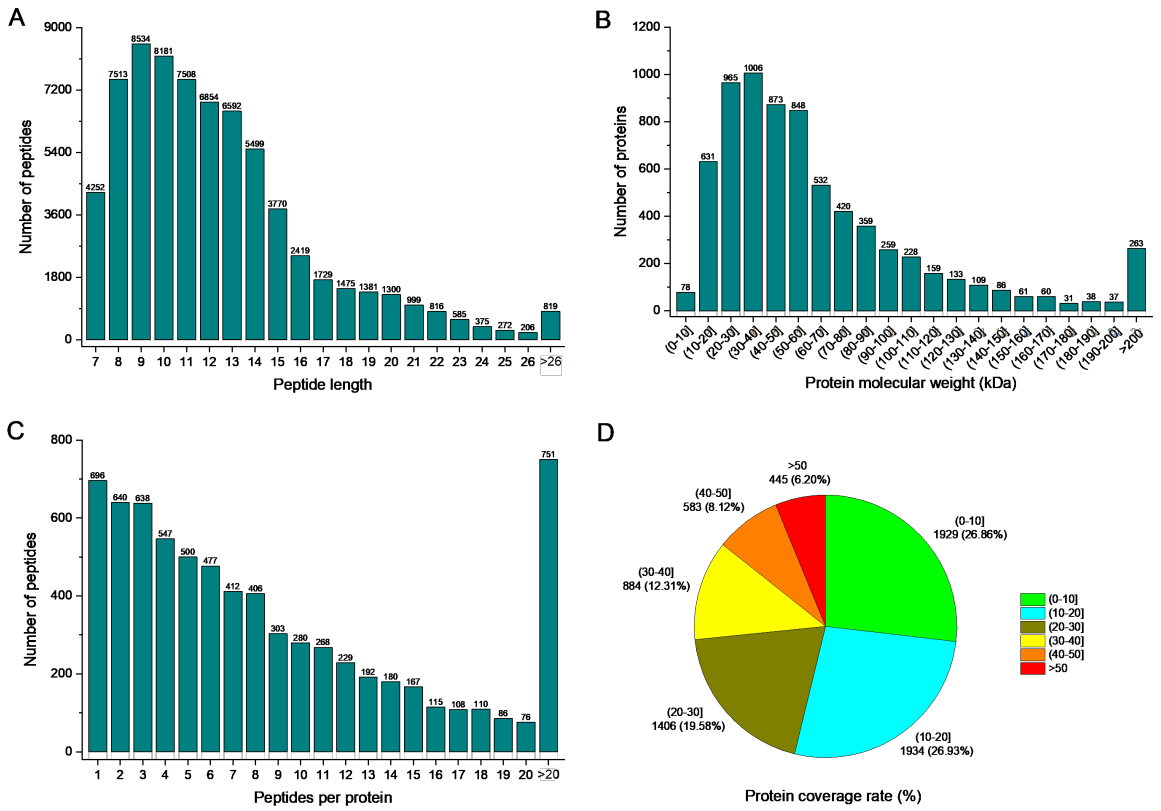

Fig. S1 General characteristics of peptides and proteins determined by sequencing. (A) Distribution of peptide length, (B) distribution of protein molecular weight, (C) distribution of peptide quantity corresponding to each protein, and (D) distribution of protein coverage rate, %.

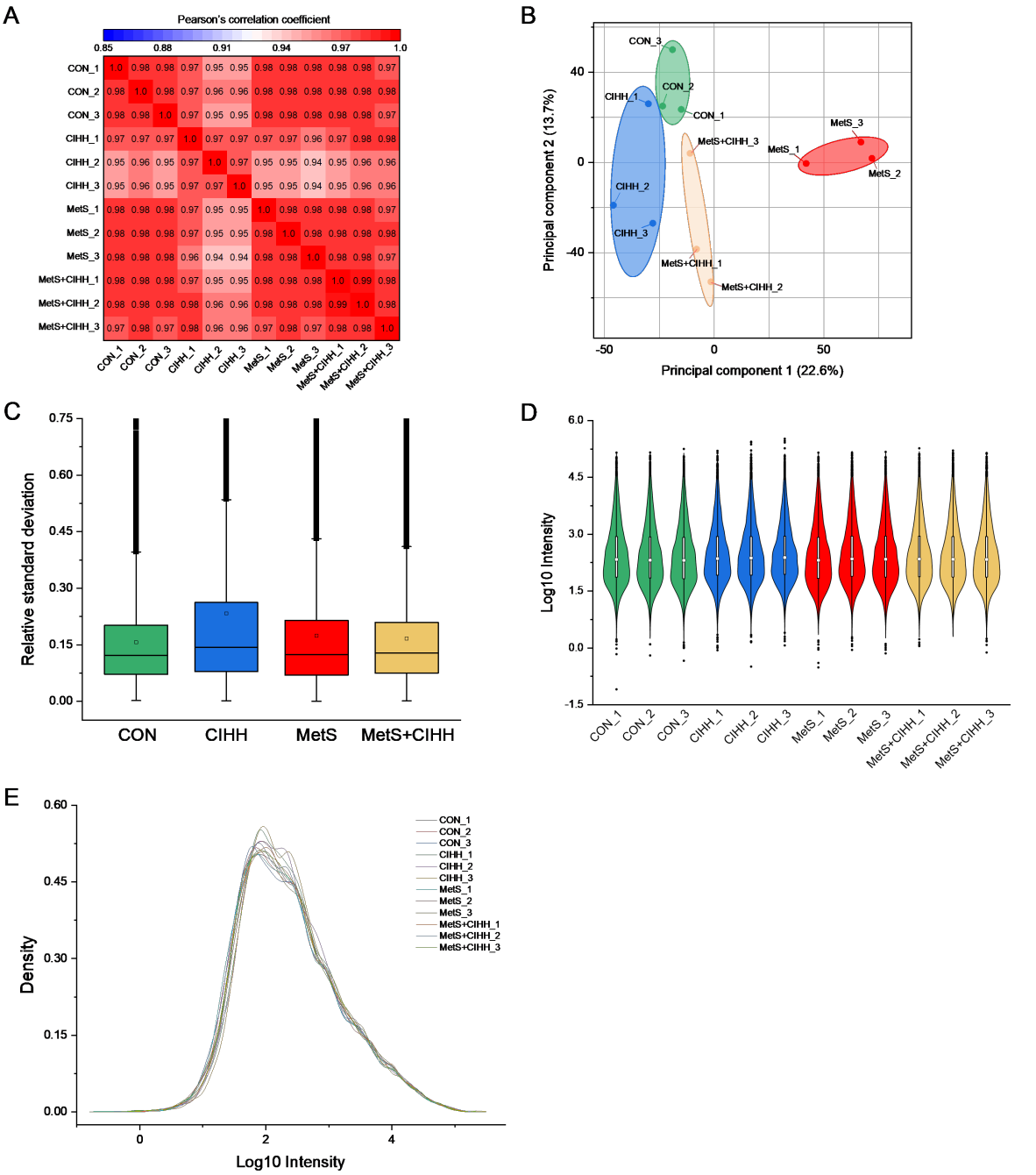

Fig. S2 The repeatability and dispersion analysis of protein samples extracted from liver tissue in healthy and MetS mice. (A) PCC, (B) PCA, (C) RSD, (D) Log10 intensity values, (E) density distribution curve. Means in a row with no letters in superscripts indicate no statistical differences.

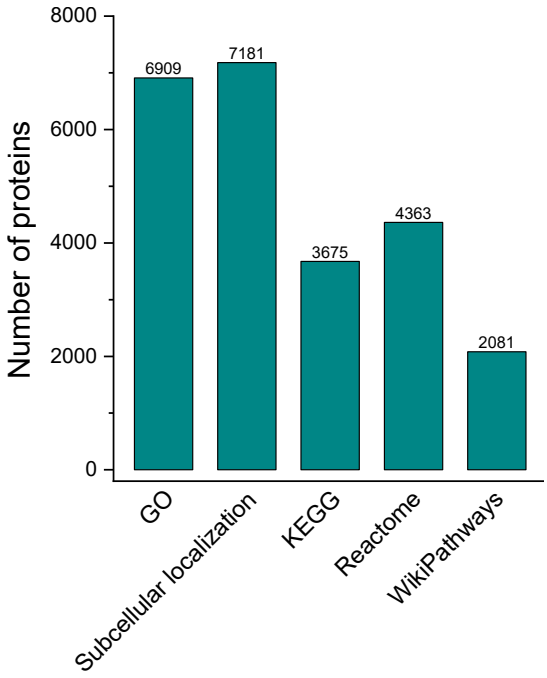

Fig. S3 The number of proteins annotated in various processes.